



**HAL**  
open science

## Very long-term incision dynamics of big rivers

Jean-Louis Grimaud, Dominique Chardon, Anicet Beauvais

► **To cite this version:**

Jean-Louis Grimaud, Dominique Chardon, Anicet Beauvais. Very long-term incision dynamics of big rivers. *Earth and Planetary Science Letters*, 2014, 405, pp.74 - 84. 10.1016/j.epsl.2014.08.021 . hal-01097322

**HAL Id: hal-01097322**

**<https://hal.science/hal-01097322>**

Submitted on 23 Dec 2016

**HAL** is a multi-disciplinary open access archive for the deposit and dissemination of scientific research documents, whether they are published or not. The documents may come from teaching and research institutions in France or abroad, or from public or private research centers.

L'archive ouverte pluridisciplinaire **HAL**, est destinée au dépôt et à la diffusion de documents scientifiques de niveau recherche, publiés ou non, émanant des établissements d'enseignement et de recherche français ou étrangers, des laboratoires publics ou privés.

1  
2  
3  
4  
5  
6  
7  
8  
9  
10  
11  
12  
13  
14  
15  
16  
17  
18  
19  
20  
21  
22  
23  
24  
25  
26  
27  
28  
29  
30  
31  
32

## Very long-term incision dynamics of big rivers

Jean-Louis Grimaud<sup>1, 2, 3, 4\*</sup>, Dominique Chardon<sup>1, 2, 3</sup>, Anicet Beauvais<sup>5</sup>

<sup>1</sup> Université de Toulouse, UPS (OMP), GET,  
14 avenue Edouard Belin, 31400 Toulouse, France

<sup>2</sup> CNRS, GET, 31400 Toulouse, France

<sup>3</sup> IRD, UR 234, GET, 31400 Toulouse, France

<sup>4</sup> now at St. Anthony Falls Laboratory,  
University of Minnesota, Minneapolis, Minnesota, USA

<sup>5</sup> Aix Marseille Université, IRD, CNRS, CEREGE UM 34  
BP 80 - 13545 Aix-en-Provence Cedex 4, France

Manuscript EPSL-D-14-00446

*Submitted 24 April 2014*

*Revised 24 July 2014*

\*Corresponding author:

E-mail address: [jgrimaud@umn.edu](mailto:jgrimaud@umn.edu)

33 **Abstract**

34           Constraining large-scale incision dynamics of shield and post-rift margin  
35 domains is key to understanding the sediment routing system over the overwhelming  
36 part of the continental surface. Based on dated and regionally correlated incision  
37 markers from West Africa, we reconstruct for the first time the entire paleo-long  
38 profiles of big rivers such as the Niger at ca. 24, 11 and 6 Ma, as well as the Eocene  
39 topography those rivers have dissected. The results provide boundary conditions and  
40 calibration for surface process models and paleodrainage dynamics. Though spatially  
41 and temporally variable, incision remained mostly below 10 m/my with a mean around  
42 5 m/my. The spatial stability of both the river outlets and divides imposed maintenance  
43 or increasing concavity of the river long profiles through time, resulting from spatially  
44 contrasted adjustment of river segments bounded by recurrent lithogenic knickzones  
45 that persisted since 24 Ma. Drainages evolved preferentially by very slow slope  
46 decrease or uniform incision in between the stationary knickzones of evolving  
47 amplitude, with apparently no relation to base level change. Therefore, knickzone height  
48 or position may not simply reflect the transient response of big rivers to base level fall  
49 as predicted by stream-power incision river models. This may also challenge uplift  
50 histories of deep continental interiors retrieved from river long profiles inversion relying  
51 on such models. Very slow incision allowed amplification of the Hoggar hot spot swell  
52 and flexural uplift of the continental margin to be recorded by river long profiles,  
53 emphasizing the potential of big non-orogenic rivers as gauges of dynamic topography.

54

55 **1. Introduction**

56           Quantifying incision dynamics of large drainage basins over geological time  
57 scales is relevant to constraining long-term landform evolution processes and the

58 responses of the sediment routing system to lithospheric deformation and climate  
59 change. Spatial and temporal variations in incision rates are mostly investigated through  
60 the study of longitudinal profiles of rivers as gauges of transient responses of landscapes  
61 to perturbations such as base level fall due to uplift. Such responses are modeled using  
62 stream-power equations and commonly integrate the formation and headward  
63 propagation of knickpoints as a mechanism of river long profile evolution (e.g.,  
64 Whipple and Tucker, 1999; Crosby and Whipple, 2006; Jeffery et al., 2013). Based on  
65 such models, an inversion procedure of river long profiles has been implemented to  
66 estimate surface uplift magnitudes (Roberts and White, 2010; Paul et al., 2014). But  
67 studies of incision processes are mostly based on modeling and/or focus on active  
68 tectonic settings over short time scales ( $10^3$ - $10^6$  yr) and face a crucial lack of regional  
69 markers of past base levels that would allow calibrating or testing incision models on  
70 Pre-Quaternary geological time scales ( $10^6$ - $10^8$  yr). This is particularly exemplified in  
71 non-orogenic settings where erosion is so slow that it may rarely be detectable by low-  
72 temperature thermochronology methods over the Cenozoic (e.g., Beauvais and Chardon,  
73 2013). Constraining large-scale incision dynamics in such settings is however key to  
74 understanding the long-term reactivity of the overwhelming part of the continental  
75 surface that supplied most of the world's passive margins and intracratonic sedimentary  
76 basins. In these tectonically "stable" contexts, river long profiles display series of major  
77 knickzones and are commonly convex downstream (Summerfield, 1991, 1996;  
78 Pazzaglia et al., 1998). These profiles pose the sizable challenge of knowing how and  
79 how fast their geometry has been acquired, how knickzones formed and evolved and  
80 what caused their convexities. If post-rift flexure of passive margins has been suggested  
81 as a cause of warping of downstream river segments (Gilchrist and Summerfield, 1990),  
82 the contributions of climatically induced sea level or erosion process changes and



83 lithospheric deformation to the acquisition of non-orogenic river long profiles are still  
84 unclear (Summerfield, 1991; Schumm, 1993; Beauvais and Chardon, 2013).

85 For the first time, we reconstruct consecutive long profiles of big rivers over  
86 their entire length since the Eocene by using the exceptional geomorphic record of  
87 successive incision stages of the West African subregion. Successive paleoprofiles  
88 allow constraining evolving rivers shapes with an emphasis on the dynamics of  
89 knickzones and are used to calibrate large-scale patterns of incision rates for three time  
90 slices over the last 24 Ma. Anomalies in river profiles are also analyzed as proxies of  
91 long wavelength lithospheric deformation.

92

## 93 **2. Geomorphic setting and incision chronology**

94 West African drainage is organized mostly around the Guinean rise and the  
95 Hoggar and Jos topographic massifs (Figure 1a). The drainage of West Africa is  
96 governed by three major river systems: the Senegal, Volta and Niger and includes  
97 shorter rivers draining the seaward slope of the Guinean rise (Figure 1a). The river long  
98 profiles are characterized by long (> 50 km), low gradient sections (i.e., 0.1 to 2 ‰)  
99 separated by knickpoints, identified as short (< 30 km) reaches of steep gradient (> 1%;  
100 Figure 1b). Two major regional knickzones made of a series of knickpoints over > 50  
101 km long river segments are recognized on most river profiles at ca. 50-100 m and 200-  
102 250 m elevation (Figures 1a and 1b).

103 West Africa is characterized by an exceptional sequence of stepped lateritic  
104 paleolandsurfaces (Figure 2), whose remnants are preserved throughout the subregion.  
105 Paleo-river long profiles were constructed by using the remnants of these  
106 paleolandsurfaces along the studied rivers (see below). In the following, the  
107 characteristics of the paleolandsurfaces are summarized after the works, among others,

108 of Vogt (1959), Eschenbrenner and Grandin (1970), Burke and Durotoye (1971),  
109 Michel (1973), Grandin (1976), Boulangé et al. (1973), Boulangé and Millot (1988) and  
110 the syntheses of Beauvais et al. (2008), Burke and Gunnell (2008) and Beauvais and  
111 Chardon (2013).

112 Relicts of surface 1 are preserved on West African summits and numerous  
113 mesas. It is a low-relief surface, which is the end product of enhanced chemical  
114 weathering that started in the Late Cretaceous and culminated in the Early Eocene to  
115 form bauxites (Figure 2). This bauxite-capped Eocene landscape, also called hereafter  
116 the bauxitic surface, represents today's envelope of the West African topography. The  
117 following paleolandsurfaces are stepped below the bauxite remnants and mark  
118 successive incision stages of the bauxitic surface (Figure 2). Surface 2, the so-called  
119 Intermediate surface, characterizes a differentiated remnant landscape coated by a thick  
120 ferricrete sealing an in-situ formed weathering mantle (Figure 2). As opposed to  
121 surfaces 1 and 2, the following three paleolandsurfaces in the sequence are pediments  
122 (glacis in the French literature): the so-called high (surface 3), middle (surface 4) and  
123 low glacis (Figure 2). The glacis surfaces commonly carry reworked bedrock and  
124 lateritic fragments derived from surfaces 1 and 2 and were, together with their cover,  
125 weathered to various degrees. Because the low glacis did not develop uniformly  
126 throughout West Africa or is commonly connected to local base levels, it was not used  
127 for paleo-long profiles reconstructions. Consequently, "surface 5" was considered as the  
128 current river levels (Figure 2). Each paleolandsurface (1 to 5) is taken as the end product  
129 of an incision period (I to V, respectively; Figure 2). Our study focuses on incision  
130 periods III to V and allows visualizing the amount of dissection of the Eocene  
131 topography during erosion period II.

132 Age constraints on the shaping, weathering and abandonment of the successive  
133 paleosurfaces in the West African sequence were obtained from radiometric  $^{39}\text{Ar}$ - $^{40}\text{Ar}$   
134 dating of supergene K-Mn oxides (i.e., cryptomelane) in the weathering profiles of each  
135 paleosurface from the Tambao type locality (Figure 1a) in Burkina Faso (synthesis in  
136 Beauvais and Chardon, 2013). Surface and core samples were taken at various  
137 elevations and depths spanning the altitudinal range of the paleolandsurfaces (Hénocque  
138 et al., 1998; Colin et al., 2005; Beauvais et al., 2008). Paleosurfaces 1 to 4 yielded  $^{39}\text{Ar}$ -  
139  $^{40}\text{Ar}$  age groups of 59 - 45, 29 - 24, 18 - 11 and 7-6 Ma, respectively, the Oligocene and  
140 Mid-Miocene weathering periods being also recorded by Ar-Ar dates of supergene  
141 jarosite and alunite in Southern Mali weathering profiles (Vasconcelos et al., 1994). The  
142 lower limits of the radiometric age groups date the stabilization of the weathering front  
143 established by the end of chemical weathering periods that ultimately led to duricrusting  
144 of each paleosurface in connection with their local base level (Beauvais and Chardon,  
145 2013). Therefore, ca. 45, 24, 11 and 6 Ma are interpreted as the maximum age of  
146 abandonment of each paleosurface by river incision due to climate switches from humid  
147 to seasonally dry (Beauvais and Chardon, 2013; Figure 2a). In other words, the ages of  
148 ca. 45, 24, 11 and 6 Ma are the terminal ages of paleosurfaces 1, 2, 3 and 4 respectively  
149 (Figure 2a) bracketing the incision periods separating those paleosurfaces.

150

### 151 **3. Method**

152 We construct rivers paleo-long profiles based on the identification and mapping  
153 of remnant of paleolandsurfaces S1 to S4 along the rivers courses over approximately  
154 20 km-wide corridors. This protocol is motivated by the fact that surfaces 2 and younger  
155 systematically dip towards those rivers (e.g., Figure 3). Our database of remnant  
156 lateritic paleosurfaces is that of Beauvais and Chardon (2013), which was extended to

157 encompass the selected river corridors at about 400 stations. At each station, base level  
 158 elevations corresponding to each paleolandsurface were obtained by projecting or  
 159 extrapolating paleosurface remnant elevation(s) onto a vertical straight line above the  
 160 current river trace (Figure 3b). Surface 1-bauxitic remnants were horizontally projected  
 161 (Figure 3), sometime up to 50 km from the river. Inselberg tops with higher elevation  
 162 than that of surface 2 relicts provide a minimum elevation for the bauxitic surface and  
 163 were also projected horizontally. Surface 2 relicts commonly encompass altitudinal  
 164 ranges on the slopes of bauxitic mesas (e.g., Figure 3b). The maximal and minimal  
 165 elevations of surface 2 relict(s) were horizontally projected to reflect the amplitude of  
 166 its local relief at each station (Figure 3b). Glacis form as concave upstream valley sides  
 167 of 0.2 to 10° in slope connected to the local base level (Grandin, 1976; Strudley et al.,  
 168 2006; Strudley and Murray, 2007). Thanks to their duricrusted cover, remnants of glacis  
 169 surfaces 3 and 4 have their original shape well preserved (e.g., Figure 3b). We therefore  
 170 extrapolated the downslope shape of the glacis by picking points from their surface  
 171 along a down-dip section towards the river (Figure 3b) and exponentially fitting those  
 172 points using formula:

$$173 \quad z = z_0 + H \exp^{-x/\sigma} \quad (1)$$

174 where  $x$  is the horizontal distance to the river,  $z$  is the elevation.  $z_0$  is the minimum  
 175 elevation of the considered geomorphic surface.  $\sigma$  is a measure of the exponential  
 176 reduction of elevation, i.e. a measure of inverse concavity, and  $H$  is a constant set by the  
 177 elevation amplitude of pediments surface. Base levels 3 and 4 elevation is calculated at  
 178 the river. Elevation error is estimated using the derivative:

$$179 \quad dz = dz_{srtm} + dz_0 + \exp^{-x/\sigma_{op}} dA + H_{op} \left( \frac{x}{\sigma_{op}^2} \right) \exp^{-x/\sigma_{op}} d\sigma \quad (2)$$

180 where  $dz_{srtm}$  is the absolute error of SRTM DEM (5.6 m in Africa ; Farr et al., 2007).  $\sigma$   
 181 index represents the inverse of concavity of the exponential fit and  $H_{op}$  and  $\sigma_{op}$  are the

182 optimum values given by the interpolation. Distribution of  $\sigma_{op}$  is quasi-normal and  
183 centered on 300 (Figure 4), attesting to the repeatability of the glacia shape over the  
184 study area and justifying the use of the fit formula (equation 1). At most stations, the  
185 error induced by the extrapolation of glacia base levels is smaller than the data point  
186 size (Figure 3b and 5). This, together with the little skewed distribution of  $\sigma_{op}$  (Figure 4)  
187 shows that the extrapolated paleobase levels are robust. At stations where glacia  
188 remnants are not large enough to be confidently extrapolated, the lowest elevation of the  
189 remnant the closest to the river is horizontally projected.

190         Given the long projection distance of some bauxite relicts and the fact that the  
191 bauxitic surface has a regional relief (Chardon et al., 2006), the envelope topography of  
192 the Eocene landscape was drawn passing through surface 1 elevation data points (Figure  
193 5). The curve joining the elevation of the lowest remnants of surface 2 has been drawn  
194 to represent the maximal elevation of rivers paleo-long profile 2 (Figure 5). Long  
195 profiles 3 and 4 were drawn from extrapolated surfaces 3 and 4 remnants or their  
196 projected lowest remnants. Modern profiles 5 were automatically extracted from the  
197 SRTM digital elevation model (Figure 5). Incision rates III, IV and V (representing time  
198 intervals 24-11, 11-6 and 6-0 Ma, respectively) were plotted along river profiles (Figure  
199 5). Incision rates IV and V were obtained using base levels 3, 4 and 5 at each station by  
200 integrating the elevation error resulting from the extrapolation (Figure 5). Maximum  
201 values of incision rate III are derived from the difference between paleoprofiles 2 and 3.

202         Detection and qualification of steps on paleoprofiles depend on data resolution.  
203 Analysis of the current and past long profiles allows defining knickzones as < 90 km-  
204 long river segments of more than 1% slope between two longer adjoining linear  
205 segments of 0.1 to 2‰ slopes. Knickpoints, which are sharper by definition, are only  
206 rarely detectable on the reconstructed profiles. Although the river profiles have

207 undergone long-wavelength distortion (section 5.2), their differential elevations  
208 constitute a meaningful estimate of incision. Likewise, comparing the relative geometry  
209 of short (<100 km) successive paleo-river segments is appropriate and relevant.

210

## 211 **4. Results**

212 We separate the studied river systems into four groups according to their  
213 location in the West African drainage (Figure 1). Group A includes the rivers draining  
214 the northwestern slope of the Guinean rise (Senegal and Gambia). Group B includes the  
215 short rivers draining the southern slope of the Guinean rise (Kakrima and Mano). Group  
216 C comprises the long southern rivers (Bandama, Comoé and Volta) and group D  
217 corresponds to the Niger drainage. The Niger River is divided in two segments (High  
218 and Low Niger) on both sides of the Niger inland delta (Figure 1). To facilitate the  
219 description of results, we show one representative example for each group (i.e. the  
220 Senegal, Kakrima, Volta and Niger main stream channels for groups A, B, C and D  
221 respectively) on Figure 5. The entire set of reconstructed profiles can be found in the  
222 data repositories.

223

### 224 *4. 1. Overall profiles shape and early drainage reorganization*

225 Past and modern long profiles of group A have a nearly straight, very low  
226 gradient slope across the Senegalo-Mauritanian basin (Figure 5a). Upstream parts of the  
227 profiles are steeper, generally stepped, with an increased slope (up to 0.7 ‰) for rivers  
228 draining the Western Guinean rise. Group B comprises the shortest rivers with paleo-  
229 and modern long profiles that have the steepest mean slopes (> 2 ‰) and are the most  
230 stepped (Figure 5b). The paleo and modern profiles of the Volta (group C) and Low  
231 Niger (group D) reveal a two-stage evolution. Indeed, the envelope of surface 1

232 underlines a divide whose crest lies between 200 and 750 km inland (Figures 5c and  
233 5d). Groups C and D rivers have incised this divide mostly during incision period II.  
234 This, together with the overall evolution of group A and B rivers indicates drainage  
235 reorganization during period II resulting from the dissection of an Eocene marginal  
236 upwarp that survived or was rejuvenated in the Guinean rise (Beauvais and Chardon,  
237 2013). This rearrangement involved capture of pre-45 Ma internal drainages by at least  
238 the Volta and Low Niger. More generally, depressions in the envelope of surface 1 (e.g.,  
239 Figure 5c) are indicative of transverse paleovalleys before drainage rearrangement  
240 and/or second-order captures during rearrangement (see also data repositories). The fact  
241 that the post-rearrangement, 24 Ma old surface 2 systematically dips towards the current  
242 main drains warrants calibration of post 24 Ma incision.

243         Group C profiles 2 to 5 show a nearly parallel evolution. They are made of  
244 straight, low slope ( $< 0.1 - 0.3 \text{ ‰}$ ) segments hundreds of kilometers long, which are  
245 separated by knickzones, notably those highlighted on Figure 1. Profiles 2 to 5 converge  
246 and merge towards the coast downstream of the lower regional knickzone (Figure 5b).  
247 The High Niger River shows strongly concave paleo and modern profiles (Figure 5e),  
248 whereas post-surface 1 Low Niger profiles have low and slightly convex slopes  
249 diverging downstream (Figure 5d). Paleo long profiles reveal that knickzones on  
250 modern profiles have persisted since at least profile 3 (Figure 5).

251         Analysis of geological maps shows that those recurrent knickzones coincide  
252 with lithological contrasts expressed in the topography (Figure 5). Two main contrasts  
253 are distinguished, those related to steep contacts between greenstone belts and their  
254 adjoining granite-gneiss terrains and those formed across tabular sandstones. In the first  
255 case, the knickzone horizontally encompasses the along-river width of a greenstone belt  
256 or the lower limit of the knickzone coincides with the contact between a wide

257 greenstone belt and granitogneisses. In the second case, the most common configuration  
258 is the lower limit of the knickzone coinciding with the basal unconformity of the  
259 sandstones.

260

#### 261 4. 2. *Northwestern rivers (group A)*

262 On group A rivers, post-surface 2 incision generally increases from the  
263 extremities towards the central part of the profiles resulting in an increasing concavity  
264 of the profiles through time. This is particularly the case for incision IV, and, to a lesser  
265 extent, incision III (Figure 5a). In the Guinean rise, profiles 3 and 4 show mainly  
266 convex segments, with local high incision rates (up to 20 m/my) for period IV (Figure  
267 5a). Overall, incision is rather uniform during period III and becomes more localized  
268 afterwards though accompanied by a decrease of the incision rates. Incision V is locally  
269 enhanced (up to 10 m/my) by the formation of new knickzones on profile 5 (Figure 5a).

270

#### 271 4. 3. *Short southern rivers (group B)*

272 Long (> 100 km) segments of paleoprofiles 2, 3 and 4 are convex (Figure 5b).  
273 The stepped character of the profiles is accentuated through time by the apparition of  
274 shorter convex segments, particularly during incisions IV and V. Post surface 2  
275 incisions tend to increase from the extremities towards the central part of the profiles,  
276 with locally enhanced incision during incisions IV and V that led to the formation of the  
277 modern knickzones (Figure 5b). This attests to a heterogeneous incision pattern during  
278 these periods (2 to 25 m/my), as opposed to rather distributed incision during period III  
279 (about 10 m/my in average). Incision gradients are located in between knickzones, the  
280 highest peaks being located mainly upstream. Elevation difference between surface 1



281 and the modern profiles implies a maximum incision of the slope of the Guinean rise of  
282 the order of 400 m (but equivalent to only 9 m/my over the last 45 Ma) (Figure 5b).

283

#### 284 4. 4. *Long southern rivers (group C)*

285 The overall geometry of river long profiles has been acquired since the  
286 establishment of profiles 2. The two regional knickzones systematically coincide with  
287 lithological contrasts and occurred at least since profile 3 (Figure 5c). A mean  
288 cumulated incision of less than 50 m is derived from parallel and close profiles 3 to 5.  
289 Rivers show a rather parallel evolutionary pattern of profiles 2 and 3 along the central  
290 river segment comprised between the two regional knickzones (Figure 5c). This is  
291 indicative of a rather distributed incision III of ca. 7 m/my. By contrast, lower gradient  
292 of profile 2 diverges from profile 3 downstream of the upper regional knickzone and the  
293 two profiles tend to merge towards the coast (Figure 5c). Overall, eastern rivers of  
294 group C such as the Volta become increasingly stepped with time (Figure 5c).

295

#### 296 4. 5. *Niger River (group D)*

297 Although the recurrence of the two regional knickzones is not readily  
298 documented along the Low Niger, the overall pattern of profiles 2 to 5 is roughly  
299 comparable to that of the Volta, with a diversion of the profiles downstream of the  
300 inland delta (e.g., comparison of Figures 5c and 5d). This attests to an increase in  
301 Neogene incision(s) downstream the inland delta. The overall long wavelength  
302 convexity of profiles 3 and 4 is documented between 200 and 1200 km (Figure 5d).  
303 Nearly parallel profiles 2 to 4 converge within the Iullemmeden basin. A single  
304 knickzone may be documented on profile 3 (ca. 450 km) and none may be detected on  
305 profile 4 (Figure 5d). But this may be due to the low resolution of our dataset

306 downstream of the Iullemeden basin. A two-step knickzone occurs on the modern  
307 profile between 800 and 1000 km (Figure 5d). Incision period V created high local  
308 relief compared to that of period IV, particularly downstream of the lower regional  
309 knickzone (e.g., Figure 5d). Incision V becomes limited approaching the inland delta  
310 and the coast ( $< 5$  m/my) and increases towards the central part of the profiles, with the  
311 highest incision rates downstream of the two-step knickzone of profile 5 (ca. 10 m/my  
312 during periods II, IV and V; Figure 5d).

313         Paleo long river profiles of the High Niger (Figure 5e) are comparable to those  
314 of the Senegal (group A, e.g., Figure 5a). All the profiles converge downstream and  
315 merge entering the inland delta, which is preceded by a knickzone 400 km upstream  
316 (Figure 5e). Profiles 2 to 5 may be divided in two segments i.e., a lower, ca. 1000 km  
317 long and low gradient segment of parallel profiles and an upper, very steep and short  
318 segment within the Guinean rise (Figure 5e). Most of the incision along the High Niger  
319 took place during period II (locally more than 15 m/my). Incision rates III to V are  
320 remarkably low and uniform along the lower segment ( $< 6$  m/my) and may locally  
321 attain 15 m/my in the Guinean rise (Figure 5e). The overall tendency of the upper Niger  
322 is an increase in the concavity of river profiles.

323

## 324 **5. Interpretation and discussion**

### 325 *5.1. Incision dynamics and river profiles evolution*

326         The present analysis shows that the overall shape of river profiles was acquired  
327 at least since  $\sim 11$  Ma, and most probably  $\sim 24$  Ma (Figure 6). The overall concavity of  
328 the successive river long profiles increased over the Neogene as a result of the pinning  
329 down of their two extremities (Figure 6). This attests to the horizontal stability of the  
330 divides and efficient adaptation to relative sea level change at the coast over the

331 Neogene. This very long-term divide stability, which has also been documented for the  
332 Southeastern margin of Australia (e.g., Young, 1989) contrasts with the view of  
333 drainage networks as “permanently” reorganizing in comparable passive margin  
334 contexts (Willett et al., 2014). We suggest that following drainage rearrangement  
335 (section 4.1), local relief and regional topography of West Africa acquired by the end of  
336 erosion period II had attained a threshold preventing divide migration after the  
337 Oligocene. Neogene divide stability over West Africa implies long-term stable  
338 geometry of drainage basins, which has major implications for understanding source-to-  
339 sink systems (Grimaud et al., 2014). This stability is reflected by low incision rates  
340 through space and time with more than 75 % of the data below 10 m/my and medians  
341 and means between 3 and 15 m/my (Figure 7). The last incision period would have  
342 recorded the smallest incision rates. Highest incision rates correspond to the steepest  
343 rivers draining the Guinean rise (groups A and B; Figure 7; upper Niger; Figure 5e),  
344 suggesting a control of potentially old, large-scale reliefs on incision heterogeneities  
345 (Beauvais and Chardon, 2013). To summarize, the present work provides constraints on  
346 boundary conditions and incision rates for large-scale surface process models in  
347 “stable” continental environments over geological time scales.

348         Our results reveal the long lasting maintenance of lithogenic knickzones along  
349 most rivers for at least ~11 my and most probably 24 my (Figure 6). Similar recurrent  
350 knickzones were documented in the comparable morphotectonic context of Eastern  
351 Australia (Bishop et al., 1985; van der Beek and Bishop, 2003). The concavity and  
352 stepped character of West African river long profiles have been amplified since the  
353 Early Neogene by very slow, non-uniform and unsteady incision in between stationary  
354 knickzones (Figures 5 and 6). Type-evolutionary patterns of rivers segments comprised  
355 between stationary knickzones are shown on Figure 8. Parallel evolution by strict

356 uniform incision (Figure 8a) is characteristic of the High Niger River since 24 Ma  
357 (Figures 5e and 6d). Such an evolution is also locally observed on segments of the Low  
358 Senegal, Volta and Low Niger (Figure 5a, 5c and 5d). In all cases, strict uniform  
359 incision is systematically of very low rate ( $< 5$  m/my). Strict downstream rejuvenation  
360 (Figure 8b) is not recorded by any of the studied rivers (Figure 5). Instead, knickzones  
361 may be created by differential incision (Figure 8c), as exemplified by the Senegal and  
362 Low Niger (at 1600-1800 km in Figure 5a and 400-500 km and 800-1000 km in Figure  
363 5d). However, most knickzones in West Africa have been amplified or smoothed  
364 instead of having been created since 24 Ma (Figure 5). This resulted in slope lowering  
365 of most river segments, reflecting finite incision gradients along those segments (Figure  
366 8d). This situation is best exemplified along the Senegal (at 1000-1200 km), Kakrima  
367 (at 100-300 km), Volta (600-800 km) and Low Niger (at 400-800 km and 1700-2000  
368 km) (Figure 5).

369         The above analysis indicates that knickzones do not and did not separate  
370 downstream rejuvenated from upstream relict portions of the landscape, which is  
371 implicit in models of river long profile evolution by pure knickzone retreat, particularly  
372 that originally popularized by King (1948) in the African context. River segments  
373 bounded by recurrent lithogenic knickzones evolved apparently independently from  
374 each other by preferential slope decrease or uniform incision in between nodes made by  
375 pinned knickzones of evolving amplitude. This indicates that large non-orogenic  
376 drainage basins evolve through very slow ( $< 10$  m/my) and non-uniform incision  
377 patterns that do not respond in a simple way to relative sea level change, to the  
378 exception of their lowermost reaches i.e., group C and D rivers during period IV  
379 (Figures 5 and 6, see below). In other words, repercussion of a major relative sea level  
380 drop is not likely to be recorded at a large distance from the coast in such drainages.

381 This warrants caution in using knickzones' height as a gauge of discrete uplift and  
382 figuring river profile response to uplift by headward propagation of such knickzones  
383 using stream-power river incision models. Accordingly, uplift histories retrieved from  
384 river profiles inversion procedures based on such models could be challenged,  
385 particularly those obtained for reliefs of the deep interior of the African continent (see  
386 Roberts and White, 2010 and Paul et al., 2014). As opposed to uplift, our results would  
387 argue for a dominant control of climate-driven erosion processes on incision dynamics  
388 of big non-orogenic drainages over geological time scales (Beauvais and Chardon,  
389 2013).

390

#### 391 *5.2. Anomalies in river profiles and lithospheric deformation*

392 Long wavelength (300 - 500 km long) upward convex segments of modern river  
393 profiles define a large domain comprising the Upper Volta and upper part of the Low  
394 Niger drainages (Figures 6c, 6d and 9). Our field observations and digital topographic  
395 data further indicate that this area coincides with portions of the Niger drainage that  
396 have incised their lowermost terrace. The convex river segments do not exceed 50 m in  
397 amplitude and are interpreted to reflect active transient adjustment by enhanced  
398 incision. The dynamics of two other major segments of the Niger and Volta drainage  
399 have been modified in the recent geological past. Indeed, the lower portion of the High  
400 Niger and the Gondo flew to NE before becoming alluvial plains (i.e., internal deltas)  
401 around the end of the Pliocene (Figure 9). These changes in river dynamics may result  
402 from slope decrease of those NE flowing drains. Both the upward convex river  
403 segments and internal deltas are interpreted to respond to southwestward growth of the  
404 Hoggar swell, which would be comparable to the lateral propagation of an active  
405 anticline (Keller et al., 1999), the direction and sense of propagation being determined

406 by the northeastward displacement of the African plate with respect to the Hoggar  
407 plume and/or to asthenospheric flow under the plate (Figure 9). Swell growth would  
408 induce slope decrease on the drains flowing towards the propagating swell to create  
409 internal deltas, whereas drains flowing across the propagating swell undergo enhanced  
410 incision to keep pace with growing uplift. The area of active uplift (Figure 9) mimics  
411 the domain of positive dynamic topography expected from mantle circulation models of  
412 Forte et al. (2010), reinforcing the causal link suggested here between mantle dynamics  
413 and river profiles evolution.

414 Long wavelength (500 - 1000 km) convexities of the lower part of river profiles  
415 2 to 4 are documented for drainages C and D (Figures 6c and 6d). For group C,  
416 convexity seems to increase with time (from profile 3 to profile 2) and has maximum  
417 amplitude of ca. 100 m and a wavelength of ca. 500 km. This convexity is replaced on  
418 the current profile by the lower regional knick zone and a concave lowermost portion of  
419 the rivers (Figure 6c). Warping is also documented on the lower Niger particularly on  
420 nearly parallel profiles 2 and 3, with a ca. 200 m amplitude and 1000 km wavelength  
421 convexity (Figure 6d). The convexity amplitude of profile 4 is much lower, indicating  
422 that profiles 2 and 3 underwent warping mainly before 6 Ma. The last erosion period  
423 (i.e., post 6 Ma) is also characterized by the creation of the major (double) regional  
424 knickzone and the acquisition of a concave lowermost profile (Figure 6d). Warping and  
425 post-6 Ma rejuvenation by knickzone creation of the lowermost portion of group C and  
426 D rivers are interpreted to result from flexural uplift of the continental margin (e.g.,  
427 Gilchrist and Summerfield, 1990). Flexure was enhanced by (i) the narrowness of the  
428 two transform segments of the margin in this area (Figure 9), (ii) high and increasing  
429 Neogene clastic sedimentation rates at its foot (Séranne, 1999; Jermannaud et al., 2010)  
430 and (iii) onshore denudation (Beauvais and Chardon, 2013). The 500-1000 km

431 wavelength of the flexure is too large to reflect only warping across a steep margin and  
432 is typical of asthenospheric-scale processes (e.g., McKenzie and Fairhead, 1997). We  
433 suggest that flexural uplift of the margin combined with the growth of the Hoggar swell  
434 (this work) and/or with the uplift of the continent (e.g., Burke, 1996) to produce such a  
435 wavelength.

436

### 437 *5.3. Open questions*

438       Creation or amplification of major knickzones achieves post 6 Ma rejuvenation  
439 of the warped lower portion of rivers flowing to the transform portions of the West  
440 African margin (Figure 6). The contribution, if any, of the Quaternary eustatic cycles to  
441 the creation of those knickzones may not be evaluated and whether these knickzones are  
442 actively migrating and/or evolve by knickpoint retreat should be the focus of future  
443 research. Knickpoint retreat is inferred to have been instrumental in the Plio-Pleistocene  
444 rejuvenation of the Appalachian landscape in a passive margin context comparable to  
445 that of West Africa (Gallen et al., 2013). Upstream West African drainage did not  
446 evolve by large wave(s) of headward migrating knickzones but our results are based on  
447 very long term measurements that may have averaged discrete periods of fast incision  
448 (Gardner et al., 1987). Hence, they do not allow testing whether knickpoint retreat  
449 process actually contributed to shaping individual river segments bounded by recurrent  
450 knickzones.

451       Likewise, documented distortion of portions of past river profiles poses the issue  
452 of whether rivers maintained their concavity against upwarping of abandoned base level  
453 markers or increased their overall concavity from more convex states. In the case of the  
454 lower reaches of group C and D rivers having undergone marginal flexural uplift, the  
455 first situation would clearly apply. The second situation could apply to the rest of the

456 drainage with the noticeable exception of the northern slope of the Guinean rise (group  
457 A rivers; Figures 5a and 6a). But in absence of independent geological constraints on  
458 the potential relative uplift of the rise during the Cenozoic, it is not possible to evaluate  
459 its impact on the acquisition of long river profiles of West Africa.

460

## 461 **6. Conclusions**

462         The spatial analysis of dated and regionally correlated incision markers allows  
463 calibrating incision dynamics of big West African rivers over the last 45 my and  
464 quantifying the evolution of their long profiles since 24 Ma. Incision rates are  
465 distributed spatially and remained below 10 m/my and mostly below 5 m/my. Spatial  
466 stability of both the outlets and divides of the rivers since 24 Ma imposed increasing  
467 overall concavity of their long profiles, which was achieved by contrasted adjustment of  
468 river segments separated by persistent lithogenic knickzones. River segments evolve by  
469 preferential slope decrease or uniform incision in between nodes defined by the pinned  
470 knickzones of evolving amplitude. Therefore big non-orogenic rivers do not respond  
471 simply to relative sea level change, which is unlikely to be recorded far inland in the  
472 form of purely retreating knickzones. Accordingly, knickzone height or position on such  
473 rivers are not obvious gauges of base level fall and caution is required in retrieving  
474 regional uplift histories of deep continental interiors from river long profiles inversion  
475 procedures. Rather uniform and slow incision of large non-orogenic drainage basins  
476 allows distortion and anomalies in river profiles to record subtle long wavelength  
477 surface uplift due to hot spot swell growth and flexure of continental margins,  
478 emphasizing their potential as gauges of dynamic topography.

479

## 480 **Acknowledgments**



481           This work was funded by the ANR TopoAfrica (ANR-08-BLAN-572 0247-02),  
482 the CNRS and WAXI. We thank S. Carretier, S. Bonnet, P. van der Beek and G. Hérail  
483 for fruitful discussions and Ph. Dussouillez for support. We are indebted to F. Pazzaglia  
484 for very constructive reviews. The manuscript benefited from comments by K. Burke  
485 and anonymous reviewers. We acknowledge AMIRA International and the industry  
486 sponsors, including AusAid and the ARC Linkage Project LP110100667, for their  
487 support of the WAXI project (P934A) as well as the Geological Surveys/Departments  
488 of Mines in West Africa as sponsors in kind of WAXI.  
489

490 **References**

- 491 Beauvais, A., Chardon, D., 2013. Modes, tempo and spatial variability of Cenozoic  
492 cratonic denudation: The West African example. *Geochem. Geophys. Geosyst.*  
493 14, 1590–1608, doi:10.1002/ggge.20093.
- 494 Beauvais, A., Ruffet, G., Hénocque, O., Colin, F., 2008. Chemical and physical erosion  
495 rhythms of the West African Cenozoic morphogenesis: The  $^{39}\text{Ar}$ - $^{40}\text{Ar}$  dating of  
496 supergene K-Mn oxides. *J. Geophys. Res.* 113, F04007,  
497 doi:10.1029/2008JF000996.
- 498 Bishop, P., Young, R.W., McDougall, I., 1985. Stream profile change and longterm  
499 landscape evolution. Early Miocene and modern rivers of the East Australian  
500 highland crest, central New South Wales, Australia. *J. Geol.* 93, 455-474.
- 501 Bishop, P., 1985. Southeast Australian late Mesozoic and Cenozoic denudation rates: A  
502 test for late Tertiary increases in continental denudation. *Geology* 13(7), 479-  
503 482.
- 504 Boulangé, B., Delvigne, J., Eschenbrenner, V., 1973. Descriptions morphoscopiques,  
505 géochimiques et minéralogiques des faciès cuirassés des principaux niveaux  
506 géomorphologiques de Côte d'Ivoire. *Cah. ORSTOM, sér. Géol.* V(1), 59-81.
- 507 Boulangé, B., Millot, G., 1988. La distribution des bauxites sur le craton ouest-africain.  
508 *Sci. Géol. Bull.* 41(1), 113-123.
- 509 Burke, K., 1996. The African Plate. *S. Afr. J. Geol.* 99, 339-409.
- 510 Burke, K., Gunnell, Y., 2008. The African Erosion Surface: A Continental-Scale  
511 Synthesis of Geomorphology, Tectonics, and Environmental Change over the  
512 Past 180 Million Years. *Geol. Soc. Am. Mem.* 201, 1-66.

513 Burke, K., Durotoye, B., 1971. Geomorphology and superficial deposits related to large  
514 Quaternary climatic variations in South Western Nigeria. *Z. Geomorph.* 15,  
515 430–444.

516 Chardon, D., Chevillotte, V., Beauvais, A., Grandin, G., Boulangé, B., 2006. Planation,  
517 bauxites and epeirogeny: One or two paleosurfaces on the West African margin?  
518 *Geomorphology* 82, 273-282.

519 Colin, F., Beauvais, A., Ruffet, G., Hénocque, O., 2005. First  $^{40}\text{Ar}/^{39}\text{Ar}$  geochronology  
520 of lateritic manganiferous pisolites: Implications for the Palaeogene history of  
521 a West African landscape. *Earth Planet. Sci. Lett.* 238(1-2), 172-188. doi:  
522 10.1016/j.epsl.2005.06.052.

523 Crosby, B.T., Whipple, K.X., 2006. Knickpoint initiation and distribution within fluvial  
524 networks: 236 waterfalls in the Waipaoa River, North Island, New Zealand.  
525 *Geomorphology* 82, 16-38.

526 Eschenbrenner, R., Grandin, G., 1970. La séquence de cuirasses et ses différenciations  
527 entre Agnibiléfrou et Diébougou (Haute-Volta). *Cah. ORSTOM, Sér. Géol.*  
528 2(2), 205-246.

529 Farr, T.G., Rosen, P.A., Caro, E., Crippen, R., Duren, R., Hensley, S., Kobrick, M.,  
530 Paller, M., Rodriguez, E., Roth, L., Seal, D., Shaffer, S., Shimada, J., Umland,  
531 J., Werner, M., Oskin, M., Burbank, D., Alsdorf, D., 2007. The Shuttle Radar  
532 Topography Mission. *Rev. Geophys.* 45, RG2004.

533 Forte, A.M., Quéré, S., Moucha, R., Simmons, N.A., Grand, S.P., Mitrovica, J.X.,  
534 Rowley, D.B., 2010. Joint seismic–geodynamic–mineral physical modelling of  
535 African geodynamics: A reconciliation of deep-mantle convection with surface  
536 geophysical constraints. *Earth Planet. Sci. Lett.* 295, 329-341.

537 Gallen, S.F., Wegmann, K.W., Bohenstiehl, D.R., 2013. Miocene rejuvenation of  
538 topographic relief in the Southern Appalachians. *GSA Today* 23(2), 4-10,  
539 doi:10.1130/GSATG163A.1.

540 Gardner, T.W., Jorgensen, D.W., Shuman, C., and Lemieux, C.R., 1987. Geomorphic  
541 and tectonic process rates: Effects of measured time interval, *Geology* 15(3),  
542 259-261, doi:10.1130/0091-7613(1987)15<259:GATPRE>2.0.CO;2.

543 Gilchrist, A.R., Summerfield, M.A., 1990. Differential denudation and flexural isostasy  
544 in formation of rifted-margin upwarps. *Nature* 346, 739-742.

545 Grandin, G., 1976. Aplanissements cuirassés et enrichissement des gisements de  
546 manganèse dans quelques régions d'Afrique de l'Ouest. *Mém. ORSTOM* 82,  
547 Paris, France.

548 Grimaud, J.-L., Chardon, D., Rouby, D., Beauvais, A., 2014. Quantifying denudation of  
549 the West African passive-transform margin: implications for Cenozoic erosion  
550 budget of cratons and source-to-sink systems. *Geophys. Res. Abstr.* 16,  
551 EGU2014-9913.

552 Hénocque, O., Ruffet, G., Colin, F., Féraud G., 1998.  $^{40}\text{Ar}/^{39}\text{Ar}$  dating of West African  
553 lateritic cryptomelanes. *Geochim. Cosmochim. Acta* 62(16), 2739-2756.

554 Jeffery, M.L., Ehlers, T.A., Yanites, B.J., Poulsen, C.J., 2013. Quantifying the role of  
555 paleoclimate and Andean Plateau uplift on river incision. *J. Geophys. Res.*  
556 *Earth Surf.* 118, 852-871. doi: 10.1002/jgrf.20055.

557 Jermannaud P., Rouby, D., Robin, C. Nalpas, T., Guillocheau, 2010. Plio-Pleistocene  
558 Sequence Stratigraphic architecture of the eastern Niger delta: a record of  
559 eustasy and aridification of Africa. *Mar. Pet. Geol.* 27, 810-821

560 Keller, E.A., Gurrola, L., Tierney, T.E., 1999. Geomorphic criteria to determine the  
561 direction of lateral propagation of reverse faulting and folding. *Geology* 27,  
562 515-518.

563 King, L.C., 1948. On the age of African land-surfaces. *Q. J. Geol. Soc. London* 104,  
564 439-459.

565 McKenzie, D., Fairhead, D., 1997. Estimates of the effective elastic thickness of the  
566 continental lithosphere from Bouguer and free air gravity anomalies. *J.*  
567 *Geophys. Res.* 102, 27523-27552.

568 Michel, P., 1973. Les bassins des fleuves Sénégal et Gambie : étude géomorphologique.  
569 Mém. ORSTOM 63, Paris, France.

570 Paul, J.D., Roberts, G.G., White, N., 2014. The African landscape through space and  
571 time. *Tectonics* 33(6), 898-935, doi:10.1002/2013TC003479.

572 Pazzaglia, F.J., Gardner, T.W., Merritts, D.J., 1998. Bedrock fluvial incision and  
573 longitudinal profile development over geologic time scales determined by  
574 fluvial terraces, in: J. Tinkler, Wohl, E. (Eds.), *Rivers Over Rock: Fluvial*  
575 *Processes in Bedrock Channels*, *Geophys. Monogr. Ser.*, vol. 107. AGU,  
576 Washington, DC, pp. 207-235.

577 Roberts, G.G., White, N., 2010. Estimating uplift rate histories from river profiles using  
578 African examples. *J. Geophys. Res. Solid Earth* 115, B02406.

579 Schumm, S.A., 1993. River response to baselevel change: Implications for sequence  
580 stratigraphy. *J. Geol.* 101, 279-294.

581 Séranne, M., 1999. Early Oligocene stratigraphic turnover on the West Africa  
582 continental margin: a signature of the Tertiary greenhouse-to-icehouse  
583 transition? *Terra Nova* 11(4), 135-140.

- 584 Strudley, M.W., Murray, A.B., 2007. Sensitivity analysis of pediment development  
585 through numerical simulation and selected geospatial query. *Geomorphology*  
586 88, 329-351.
- 587 Strudley, M.W., Murray, A.B., Haff, P.K., 2006. Emergence of pediments, tors, and  
588 piedmont junctions from a bedrock weathering–regolith thickness feedback.  
589 *Geology* 34, 805-808.
- 590 Summerfield, M.A., 1991. *Global geomorphology; an introduction to the study of*  
591 *landforms*. Longman Scientific & Technical, Harlow, UK.
- 592 Summerfield, M.A., 1996. Tectonics, geology and long-term landscape development,  
593 in: W.M. Adams, A.S. Goudie, R. Orme, A. (Eds.), *The Physical Geography of*  
594 *Africa*. Oxford University Press, Oxford, UK, pp. 1-17.
- 595 van der Beek, P., Bishop, P., 2003. Cenozoic river profile development in the Upper  
596 Lachlan catchment (SE Australia) as a test of quantitative fluvial incision  
597 models. *J. Geophys. Res.* 108(B6), 2309.
- 598 Vasconcelos, P. M., Brimhall, G. H., Becker, T. A., Renne, P. R., 1994.  $^{40}\text{Ar}/^{39}\text{Ar}$   
599 analysis of supergene jarosite and alunite: Implications to the paleoweathering  
600 history of the western USA and West Africa. *Geochim. Cosmochim. Acta*  
601 58(1), 401-420.
- 602 Vogt, J., 1959. Aspects de l'évolution morphologique récente de l'ouest africain. *Ann.*  
603 *Géog. Fr.* 68, 367, 193-206.
- 604 Whipple, K.X., Tucker, G.E., 1999. Dynamics of the stream-power river incision  
605 model; implications for height limits of mountain ranges, landscape response  
606 timescales, and research needs. *J. Geophys. Res.* 104 (B8), 17661–17674,  
607 doi: 10.1029/1999JB900120.

- 608 Willett, S.D., McCoy, S.W., Perron, T.J., Goren, L., Chen C-Y., 2014. Dynamic  
609 reorganization of river basins. *Science* 343, 1248765,  
610 doi:10.1126/science.1248765.
- 611 Young, R.W., 1989. Crustal constraints on the evolution of the continental divide of  
612 eastern Australia. *Geology* 17, 528-530.
- 613

614 **Figure captions**

615

616 **Figure 1.** (a) Topography, drainage and selected geologic and geomorphic features of  
617 West Africa. Topography is derived from smoothing of the Shuttle Radar Topography  
618 Mission DEM to 5 km resolution. Thick grey lines labeled 1 and 2 refer to the lower  
619 and upper regional knickzones, respectively. Capital letters refer to the studied groups  
620 of rivers. A – northwestern rivers (long profiles shown in Figure 5a); B – short southern  
621 rivers (Figure 5b); C – long southern rivers (Figure 5c); D – Niger River (Figure 5d). (b)  
622 Modern long profiles of selected rivers. The lower and upper regional knickzones’  
623 elevation ranges are indicated by dark and light grey bands numbered 1 and 2,  
624 respectively.

625

626 **Figure 2.** Lateritic paleolandsurface sequence and incision chronology of West Africa  
627 (synthesized after Michel, 1973; Beauvais et al., 2008; Beauvais and Chardon, 2013).

628

629 **Figure 3.** Example of a typical field station used to estimate local paleo-base levels  
630 (Station 11 along the Bafing, corresponding to the upper Senegal River; Figures 1a and  
631 5a). (a) Google Earth view (left) with its geomorphic interpretation (right). (b) Cross-  
632 section drawn on Figure 3a showing the distribution of lateritic paleolandsurface relicts  
633 and the method by which they are projected or extrapolated above today’s river courses.

634

635 **Figure 4.** Distribution of the optimum inverse concavity  $\sigma_{op}$  in the exponential fits of  
636 pediment surfaces 3 and 4.

637



638 **Figure 5.** Reconstructed paleo- and modern river long profiles and corresponding  
639 incision rates. For each river group, the case of the most representative river is shown.  
640 (a) Northwestern rivers (group A). (b) Short southern rivers (group B). (c) Long  
641 southern rivers (group C). (d) Low Niger River (group D). (e) High Niger River (group  
642 D). Paleoprofiles 2 are overestimated in elevation. Rivers and river groups are located  
643 on Figure 1a. The complete set of river long profiles may be found in the data  
644 repository.

645

646 **Figure 6.** Synthetic representation of the successive West African paleo-long river  
647 profiles. (a) Northwestern rivers (group A). (b) Short southern rivers (group B). (c)  
648 Long southern rivers (group C). (d) Niger River (group D) (location of river groups on  
649 Figure 1a). Spiked segments of modern profiles correspond to > 300 km long upward-  
650 convex segments (mapped in Figure 9). Elevation ranges of the lower and upper  
651 regional knickzones are shown in grey and numbered 1 and 2, respectively.

652

653 **Figure 7.** Statistical summary (box and whiskers plots) of incision rates over West  
654 Africa during periods III, IV and V (24-11, 11-6 and 6-0 Ma, respectively) for each  
655 river group. Incision rates III are maximum values (see text for explanation). Incision  
656 rates IV and V are calculated using the mean elevation of base levels 3, 4 and 5 where  
657 available. Note that incision rates for period V may be slightly underestimated,  
658 particularly on the lower course of rivers C and D, where a small number of stations are  
659 available on profile 4 but where locally large incision V occurs around modern  
660 knickzones.

661

662 **Figure 8.** Type evolutions of long river profile segments comprised between two  
663 stationary knickzones (grey vertical stripes) and corresponding finite incision patterns  
664 (vertical arrows). 1 – early river profile (green); 2 – late river profile (orange). (a)  
665 Parallel evolution by uniform incision. (b) Knickpoint creation by downstream  
666 rejuvenation. (c) Knickpoint creation by differential incision. (d) Slope decrease from  
667 incision gradient.

668

669 **Figure 9.** Distribution of the main anomalies in the modern river long profiles of West  
670 Africa and its interpretation in terms of long-wavelength lithospheric deformation of  
671 mantle origin. Red arrows represent directions of horizontal propagation of the uplift  
672 wave. Northeastward extensions of the Romanche (R) and St-Paul (SP) fracture zones  
673 constitute the two main transform segments of the continental margin.

**Highlights:**

- Reconstructed long profiles calibrate very slow incision (5 m/my) since Oligocene
- Profiles pinned-down at divide, outlet and stationary lithogenic knickzones
- Flexural uplift / dynamic topography mapped from profiles convexities & anomalies

**Keywords:**

River long profiles; incision dynamics; knickzones; non-orogenic; Cenozoic; Africa

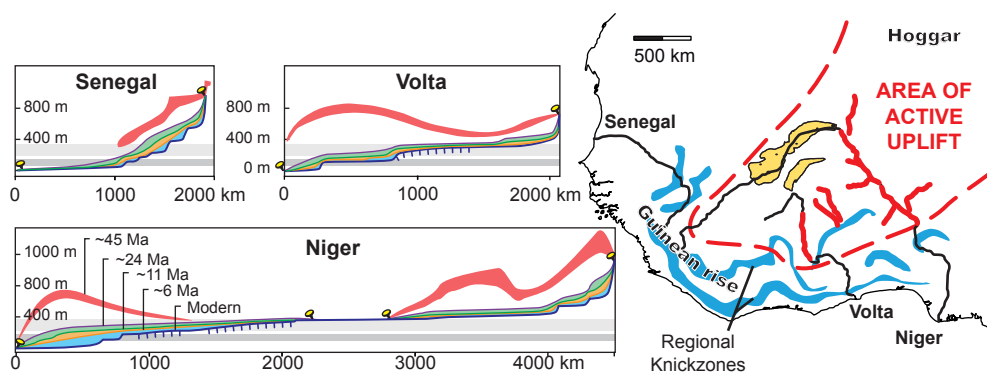
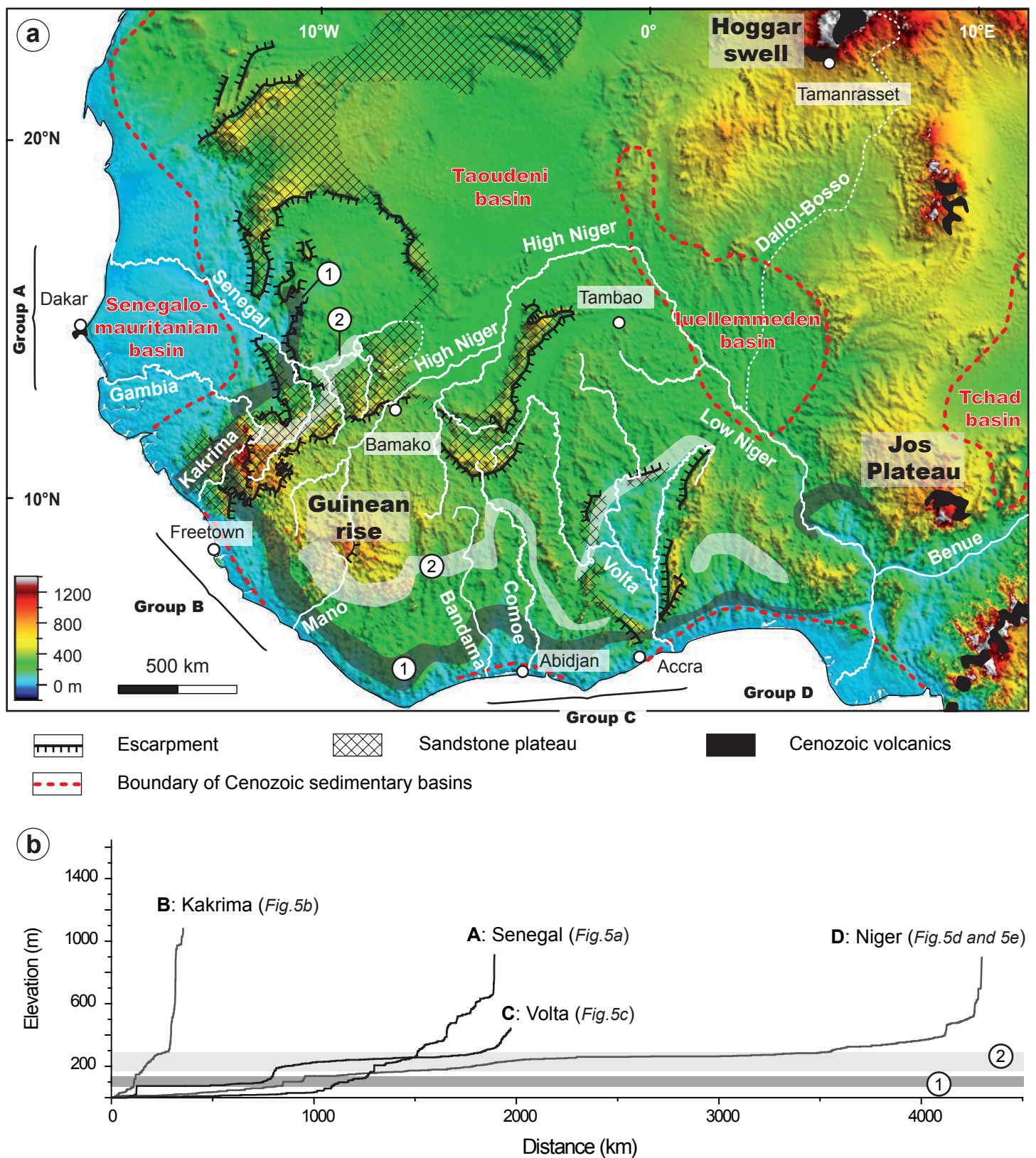
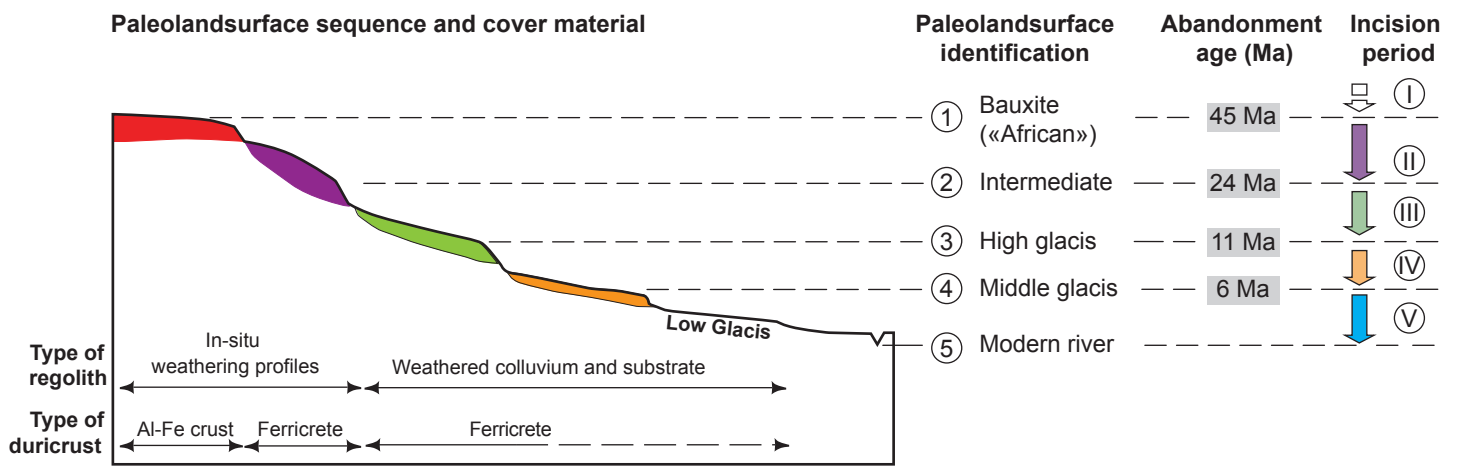


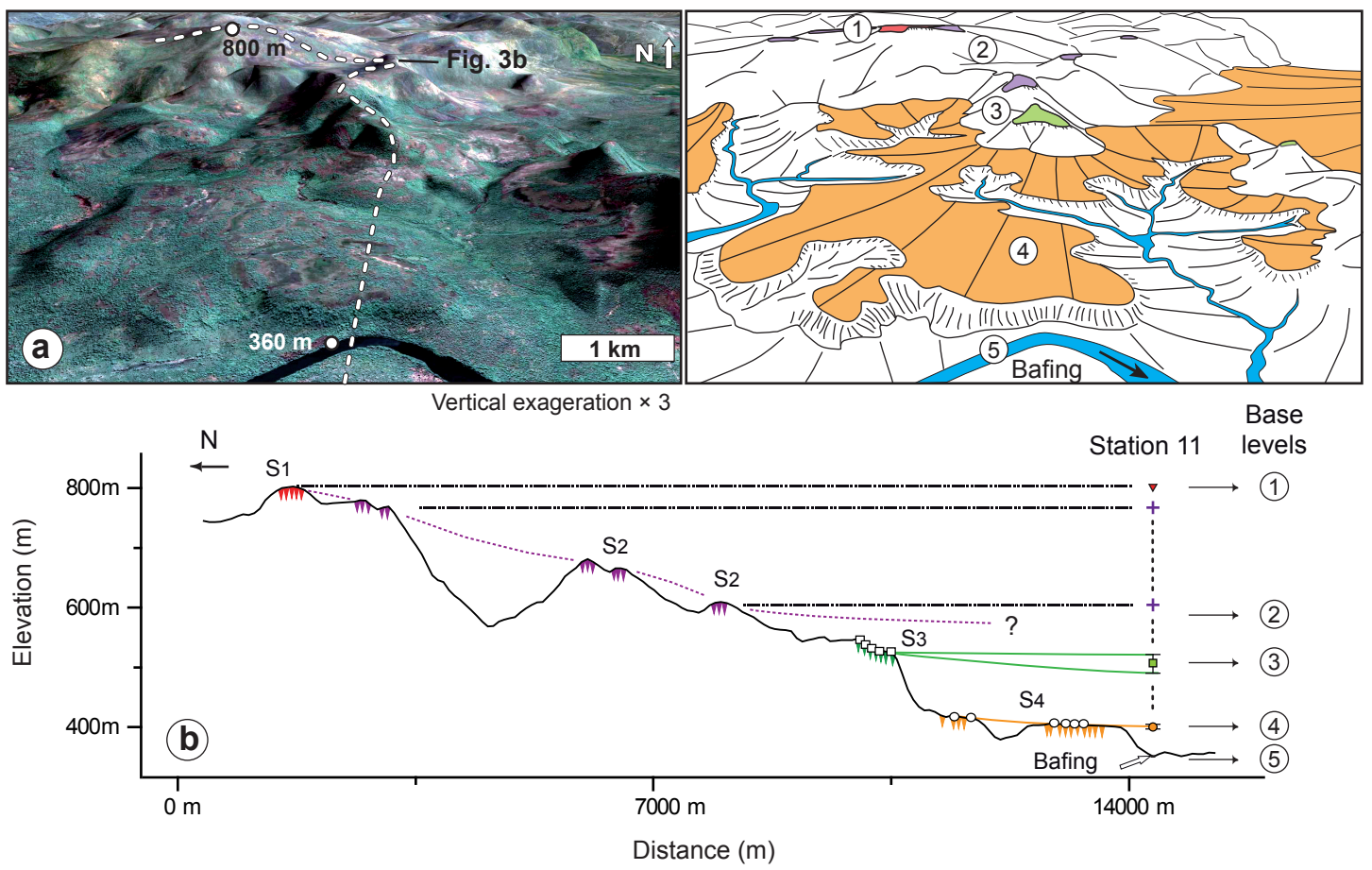
Figure 1  
[Click here to download Figure: Fig1.pdf](#)



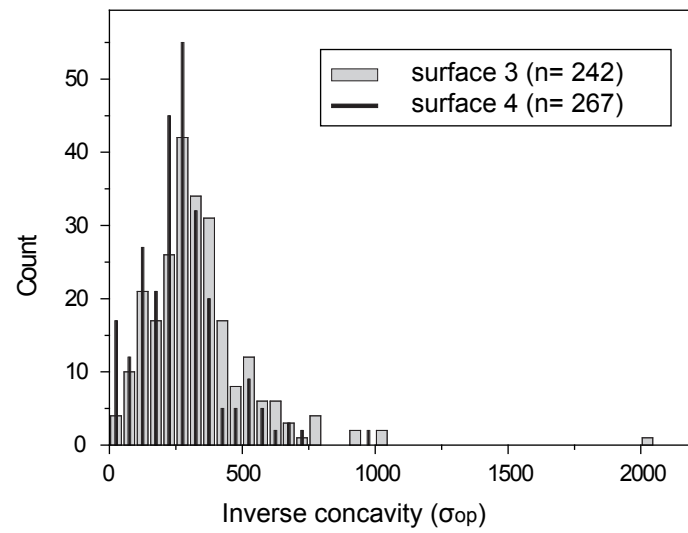
Grimaud et al., Figure 1



Grimaud et al., Figure 2



Grimaud et al., Figure 3

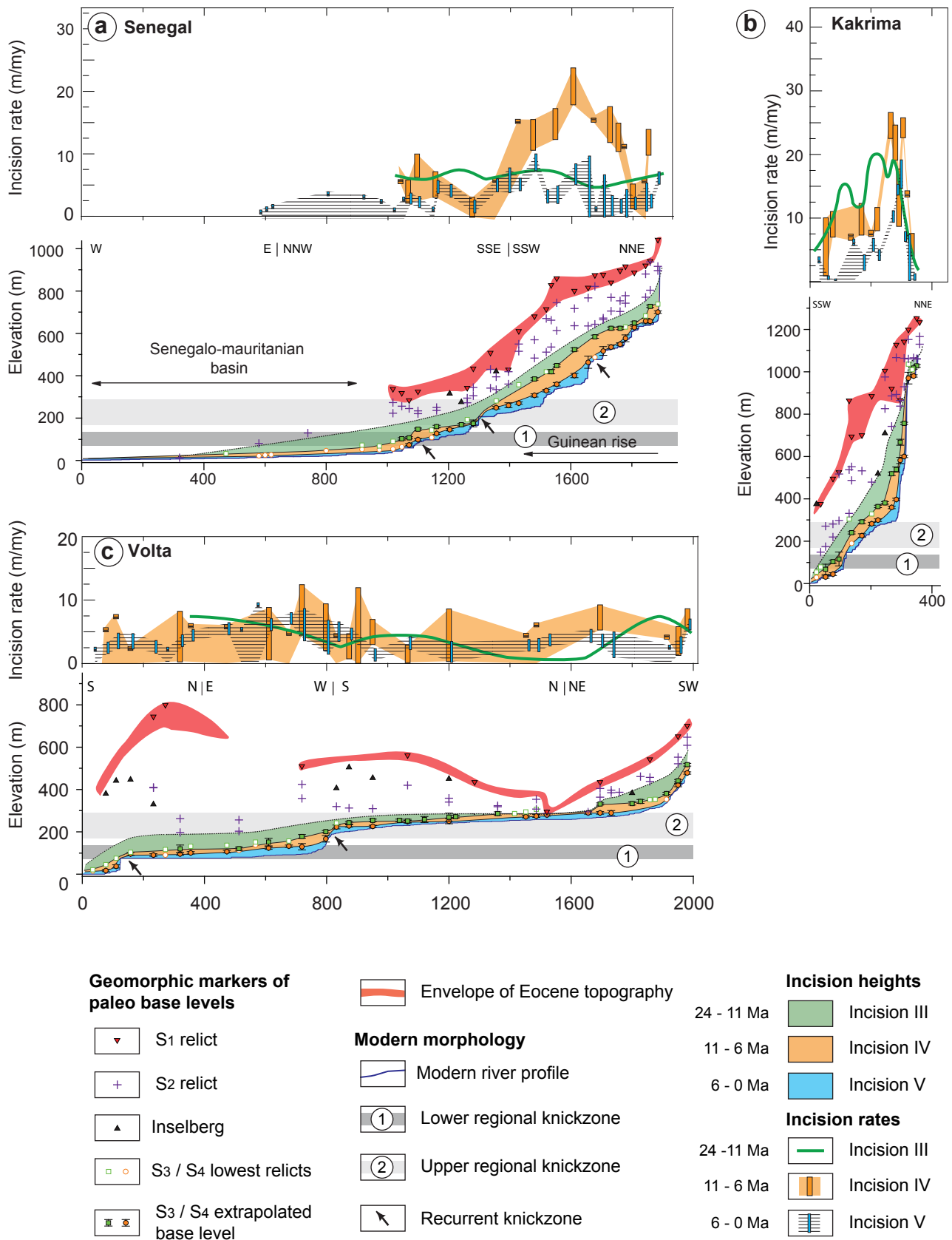


Grimaud et al., Figure 4

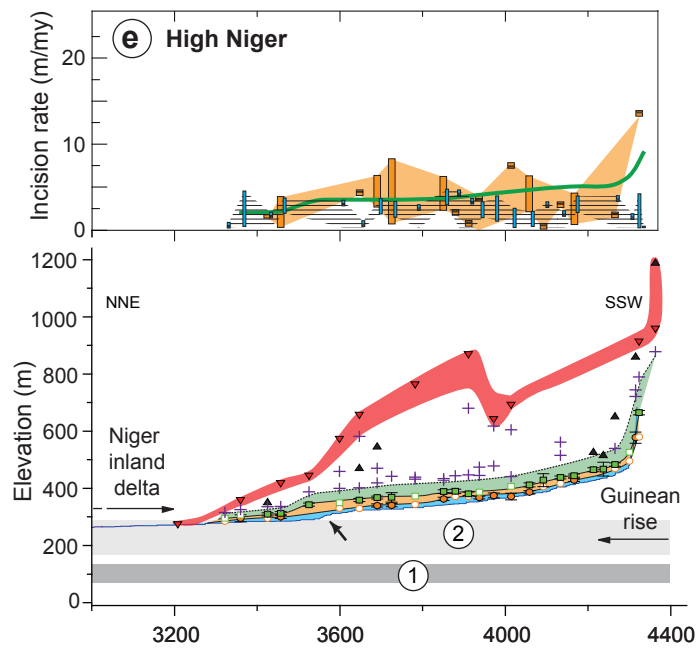
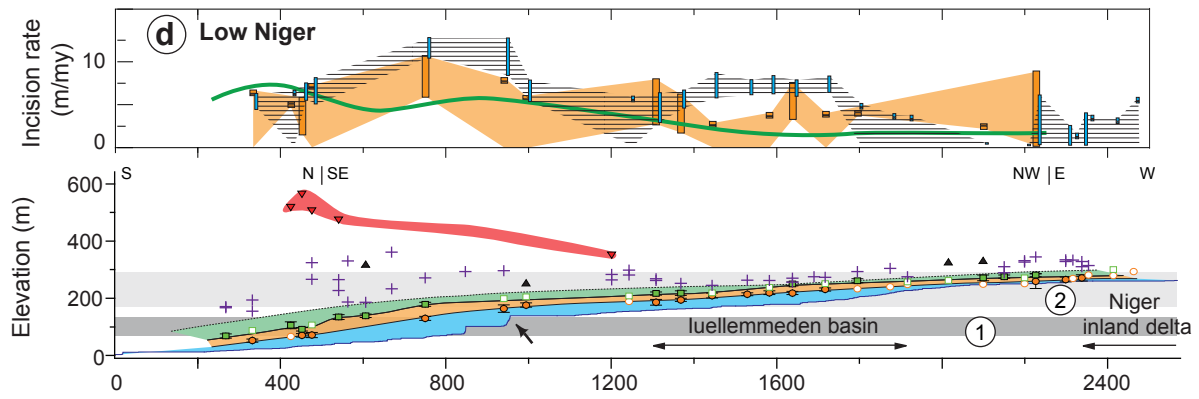


Figure 5

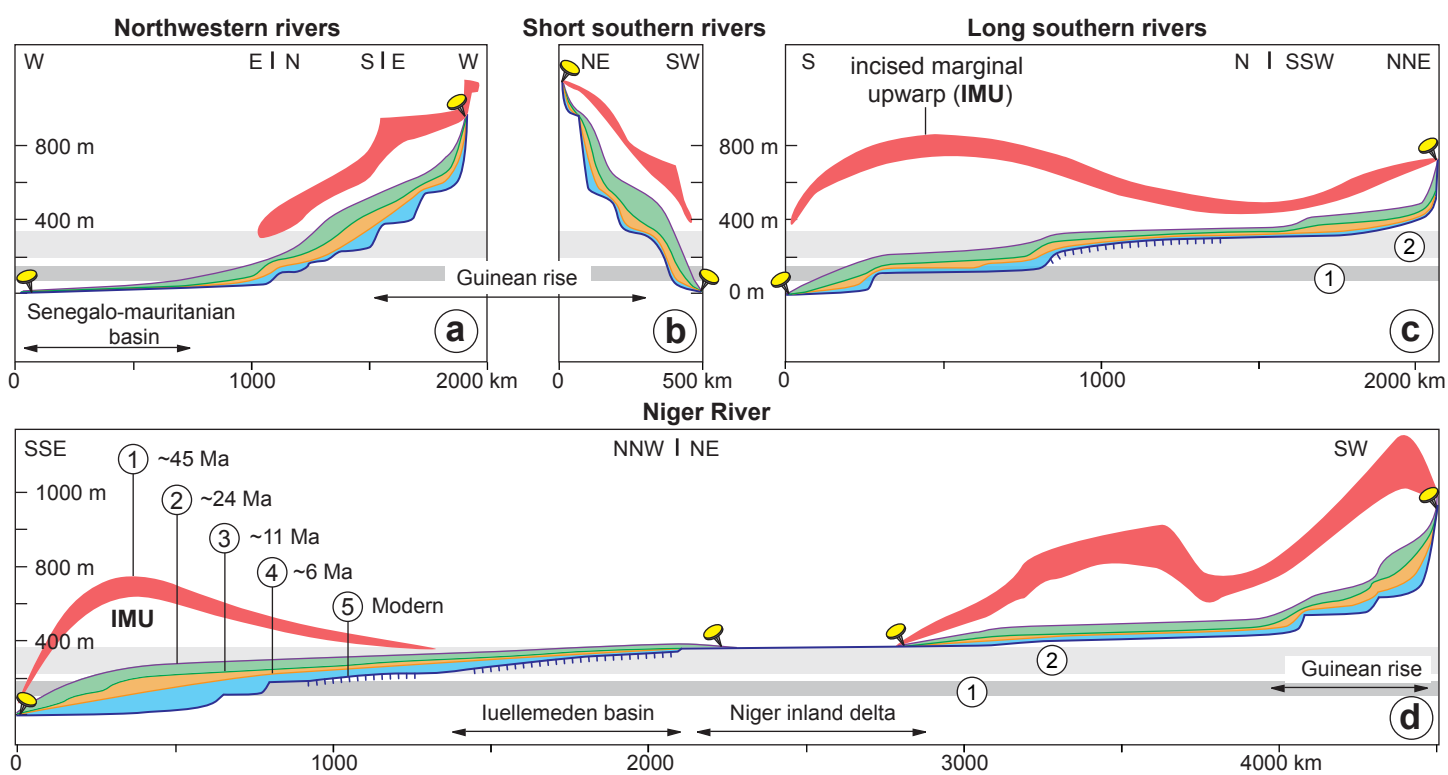
[Click here to download Figure: Fig5.pdf](#)



Grimaud et al., Figure 5

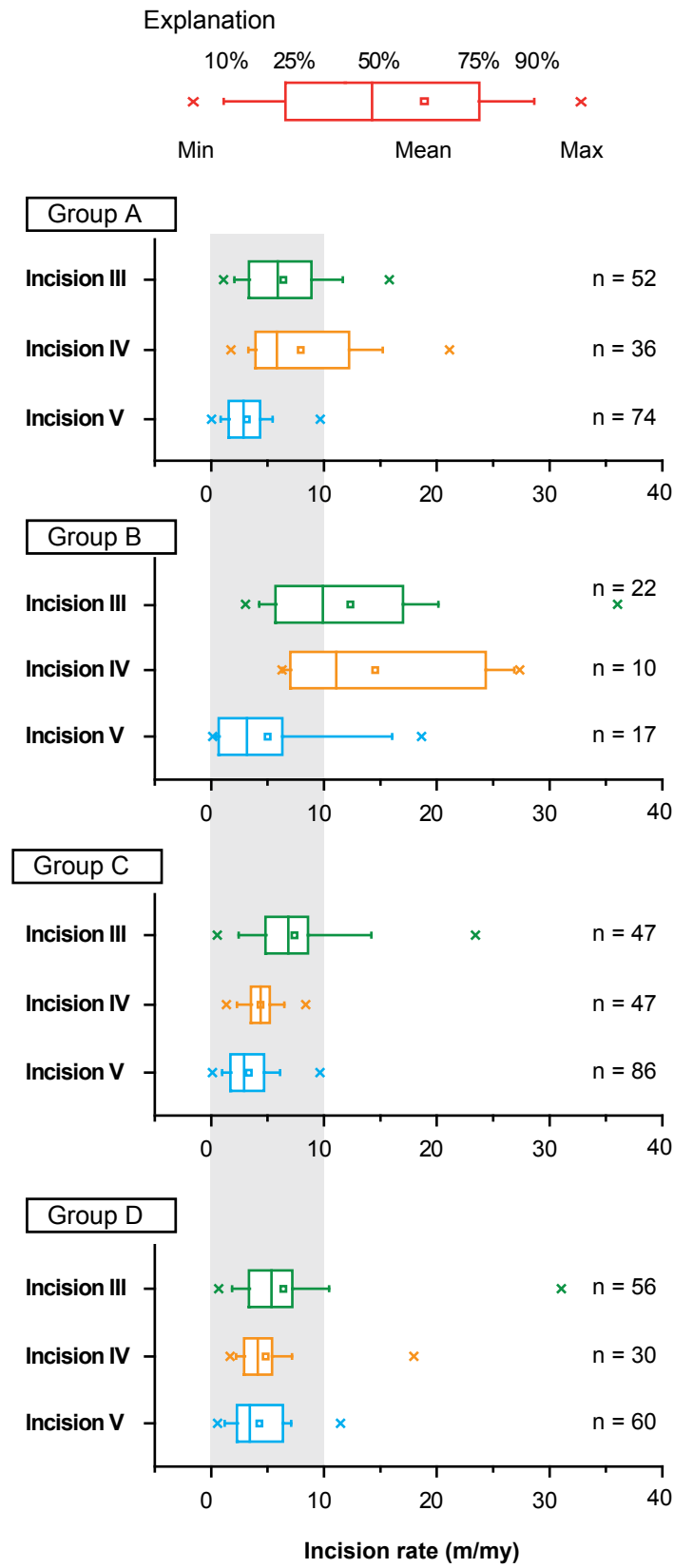


**Figure 6**  
[Click here to download Figure: Fig6.pdf](#)

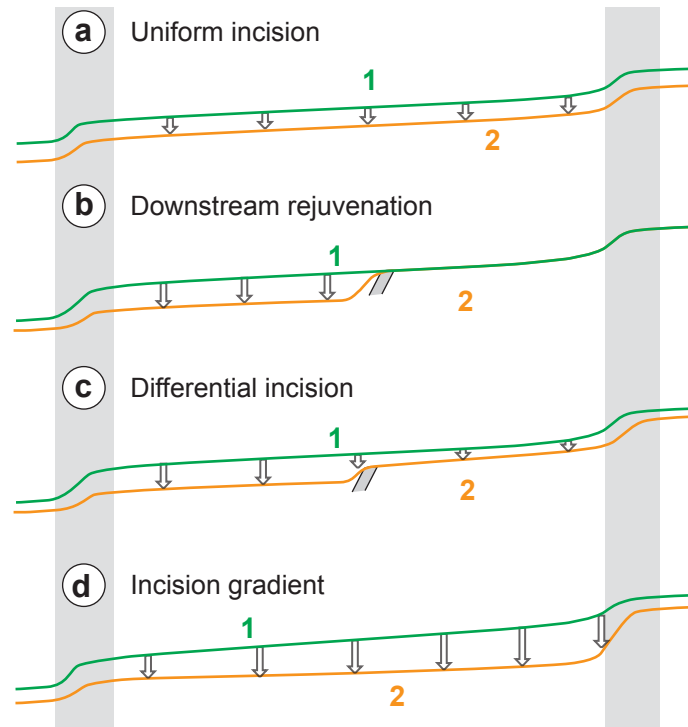


**Grimaud et al., Figure 6**

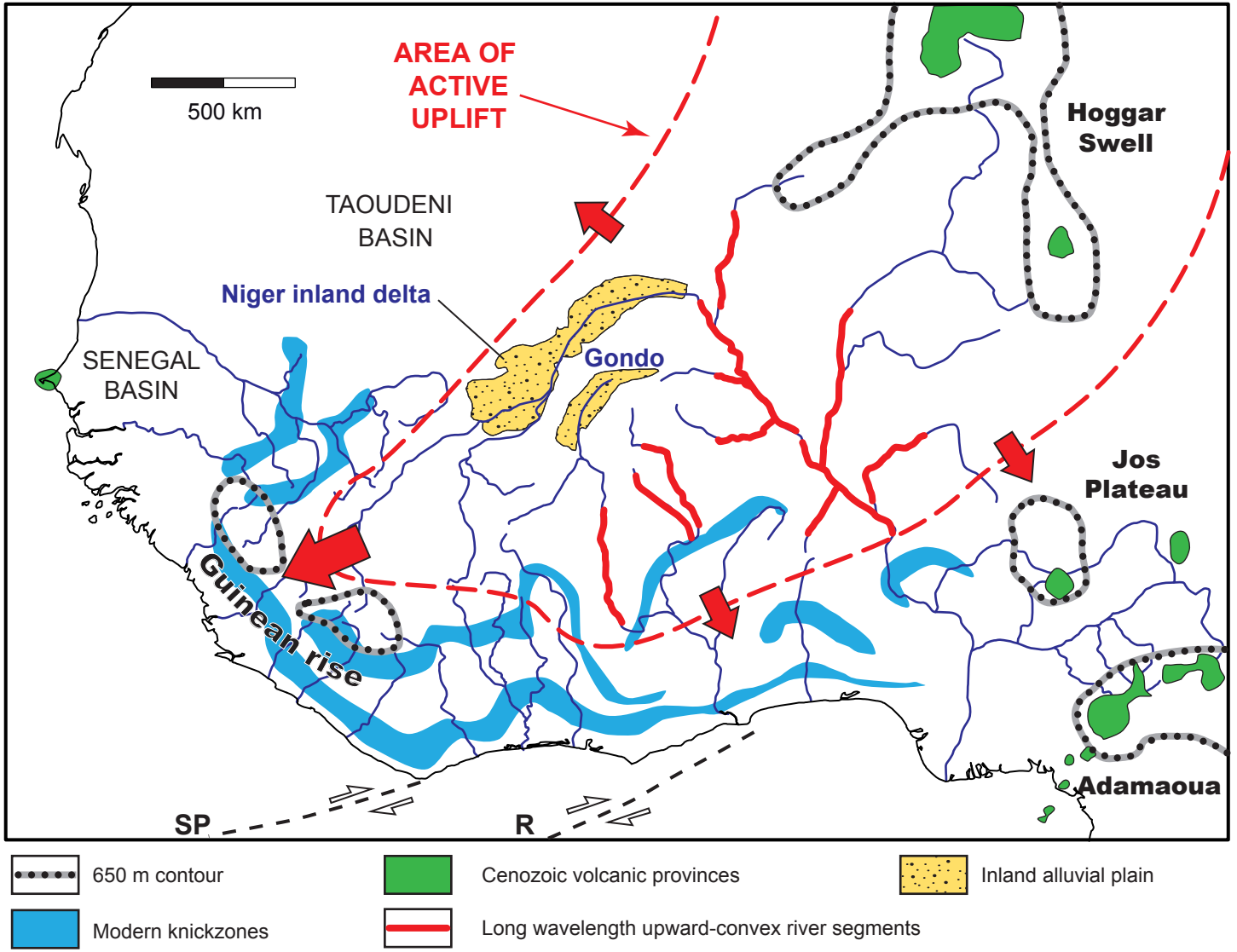
Figure 7  
[Click here to download Figure: Fig7.pdf](#)



Grimaud et al., Figure 7



Grimaud et al., Figure 8



Grimaud et al., Figure 9

**Supplementary material for on-line publication only**

[Click here to download Supplementary material for on-line publication only: DataRepository.pdf](#)